

# Prediction of Cutting Force for Milling of Inconel 718 under Cryogenic Condition by Response Surface Methodology

Nurul Hayati Abdul Halim<sup>1,2</sup>, Che Hassan Che Haron<sup>1\*</sup>,  
Jaharah Abdul Ghani<sup>1</sup>, Muammar Faiq Azhar<sup>1</sup>

<sup>1</sup>Department of Mechanical and Material Engineering,  
Faculty of Engineering and Built Environment,  
Universiti Kebangsaan Malaysia, 43600, Bangi, Selangor, Malaysia  
\*Corresponding author E-mail: chase@ukm.edu.my

<sup>2</sup>Faculty of Mechanical Engineering, Universiti Teknologi MARA, 40450,  
Shah Alam, Selangor, Malaysia

## ABSTRACT

*In order to identify the influence of different cutting parameters on cutting force under cryogenic cooling assistance, this paper presents an experimental investigation on the influence by high-speed milling Inconel 718 using carbide coated ball nose milling inserts. For Design of Experiment (DOE), Box-Behnken Response Surface Methodology (RSM) with 29 experiments was applied to accommodate 4 factors; cutting speed: 120-140 m/min, feed rate: 0.15-0.25 mm/tooth, axial depth of cut: 0.3-0.7 mm, and radial depth of cut: 0.2-0.6 mm at three levels each. The milling process was performed under a CO<sub>2</sub> cryogenic environment using a new design of cryogenic controlling system for consistent and efficient cooling effect at the cutting zone. The experimental results found the forces varied from as low as 112 N up to a maximum of 452 N. The analysis of variance (ANOVA) confirmed the axial depth of cut as the dominant factor influencing the cutting forces followed by the interaction between feed rate and radial depth of cut. The forces were significantly increased with the axial depth of cut due to the increase of the size of cut by the insert. Meanwhile, the developed statistical equation model reported an average error of 4.72% between the predicted and actual cutting forces. With 95.28% of confidence level, this confirms the adequacy of the predictive model to be used within the range of the investigated parameters. Thereby, the numerical optimization suggested*

parameters of  $V_c$ : 140 m/min,  $f_z$ : 0.25 mm/tooth,  $a_p$ : 0.3 mm, and  $a_e$ : 0.21 mm to be applied to achieve a cutting force as low as 117.72 N. The correlation between the cutting forces along with tool wear progress and pattern was also discussed.

**Keywords:** Inconel 718; Cryogenic Machining; Response Surface Methodology; Coated Tungsten Carbide; Milling

## Introduction

In aviation engine industry, Inconel 718 plays an important role as one of the important materials used for fabricating components at the hottest area of gas turbine engines [1]. This nickel-based superalloy possesses very high-temperature strength due to high melting point up to 1300 °C, and good resistance to chemical degradation that allows it to maintain its mechanical properties at extreme temperature and pressure working environment. However, Inconel 718 also has low thermal conductivity and specific heat volume that hinders its machinability [2]. Researchers such as Courbon et al. (2013), Kasim et al. (2013), Patil et al. (2014) and Zhang et al. (2012) generally reported that machining Inconel 718 generates high heat that will accumulate at cutting zone and elevate cutting temperature [3]–[6]. This condition resulted with rapid increases of cutting force and tool wear rate as well as poor surface finish. Thus, the application of cutting fluids or coolants is considerably crucial in order to dissipate the generated heat away from the cutting zone and reduce the temperature. At the same time, the correct combination of machining parameters with respect to the type of cutting tool and workpiece material should be carefully identified in order to cut Inconel 718 at optimum conditions with desired manufacturing performances.

In metal cutting, cutting force is one of the important machining responses to be controlled. It is because it has a strong correlation on the functional performance of manufactured components and machining operation such as surface finish accuracy, cutting temperature, machine vibration as well as tool wear rate. Thus, a detailed understanding of the factors affecting the cutting force is vital in order to directly control those machining performances for stable and repeatable cutting process [2]. As suggested by Zhang et al. (2012), cutting forces trends can be well applied to monitor and indicate the tool wear rates for timely cutting tool replacement [6]. Yet, Kaynak et al. (2013) recommend analyzing the influence of cutting parameters on cutting forces trends in order to understand the cutting mechanisms and performance [7].

As of today, a number of studies have investigated the influence of cutting parameters and cutting environment on cutting force. Computer

simulation system and mathematical and statistical techniques are among the methods that have raised interest among researchers for optimizing and predicting the responses instead of the purely experimental approaches which are time-consuming and costly. Response Surface Methodology (RSM) is one of the broadly applied methods for accuracy and reliable analysis. It is a mathematical and statistical technique for modeling where it uses quantitative data from the experiments as the input that influences the response and generates a numerical model that can be used to optimize the response [8]. In metal cutting, RSM is used to identify the effect of multiple factors on machining performance, as well as the influence levels of every single factor on the responses. Moreover, it also helps reduce the time and cost required to conduct the experimental investigation, which is economically important. For instance, Kasim et al. (2015) applied RSM to optimize the cutting force of Inconel 718 when milling under MQL condition [9]. As reported, the most significant influence factor was the radial depth of cut (DOC). This is because, at its higher volumes discharge, it proportionally increases the size of cut per tooth and gives major influence which significantly attributes to the increase of cutting force. In the turning process, Badroush et al. (2018) applied RSM to optimize the machinability of Inconel 718 with the main focuses were on the tool life and surface finish [10]. Meanwhile, Soo et al. (2010) used 3D finite element modeling to simulate the milling process of Inconel 718 [11]. Without experimental work, they justified that cutting force significantly increases with feed rate due to the increased material removal rate. This is in line with the experimental results presented by Alauddin et al. (1998) who reported that cutting forces increased with feed rate and axial DOC, due to the increased chips load per tooth and size of cut per tooth, respectively [12]. In addition, Said et al. (2013) analyzed the effectiveness of RSM using the Taguchi method to optimize the milling parameters of Aluminum-silicon alloy [13]. They found that ANOVA and desirability criterion provided in RSM helped determine the degree of significance of each factor and optimum condition. However, the S/N ratio by the Taguchi provided a better visualization that can determine the optimum condition. Furthermore, Kadirma et al. (2008) presented how to predict milling forces using numerical solution and statistical methods for AISI P20 [14]. Besides that, Hadi et al. (2014) investigated the chips formation using finite element analysis software ThirdWave AdvantEdge [15].

Therefore, in this study, the relationship between independent factors which are; cutting speed, feed rate, axial DOC, and radial DOC and dependent response which is cutting force was analyzed using Box-Behnken RSM when high-speed milling Inconel 718 under cryogenic CO<sub>2</sub> condition. The Box-Behnken RSM was used for analysis and optimization, as it designs the experiment without combining all factors at their highest or lowest levels simultaneously [16]. This helps it eschew conducting experiments under

extreme condition, which could consequence into unsatisfactory results. The main objective is to fully employ the RSM to build an empirical mathematical modeling that can be applied to predict the variation of cutting force within the range of parameters investigated without having to conduct experimental works. This study also aims to determine the right combination of cutting parameters to produce optimum cutting force when milling Inconel 718 under cryogenic CO<sub>2</sub> condition.

## Experiment Setting And Cutting Forces Measurement

The milling process was carried out using Sumitomo carbide coated ball nose milling inserts, grade ACK 300, with its geometries as shown in Figure 1. It is a multi-coated milling insert with alternate layers of PVD TiAlN/ AlCrN to achieve a total of 3  $\mu\text{m}$  coating thickness. Its radial rake angle, axial rake angle, and approach angle are 0°, -3°, and 90° respectively. As shown in Figure 1, the insert attached to a 16-mm diameter tool holder at an overhang of 60 mm. The experimental workpiece was a block of double aged Inconel 718 with a hardness value of  $42 \pm 2$  HRC. Table 1 shows the chemical compositions of the workpiece. Before starting the experiment, the workpiece was face milled at 0.3 mm to remove the top surface, which tends to have surface irregularities and residual stress from the previous machining. The workpiece was down-end milled on a CNC milling machine model DMG 635, V Eco. Box-Behnken RSM by using Design Expert V6.0 with 29 experiments was applied to accommodate four factors at three levels each, as shown in Table 2.

The cutting force was measured and recorded using a Neo-MoMac system, developed in-house by UKM Tech. Malaysia. The system consists of a strain gauge-based dynamometer, data acquisition (DAQ), and a GUI computer display. The workpiece was fastened onto the stationary dynamometer, which was mounted on the machine working table and connected to the DAQ. The Neo-MoMac system is used to measure the multi-component force sensors in the x, y and z-axes for tangential ( $F_x$ ), radial ( $F_y$ ) and axial ( $F_z$ ) force directions respectively. The measurement was performed and recorded at the beginning of the cut using a sharp cutting edge in order to eliminate the excessive tool wear effect. To demonstrate the correlation between cutting forces and wear progression, the tool life was measured based on the maximum tool flank wear (VBmax) of the cutting edge using a toolmaker's microscope after each specific cutting paths. The cutting process was continued until the VBmax approximately reached 0.2 mm. This is to avoid excessive tool wear effect on the workpiece and machining due to the higher temperature at higher wear rate. This approach was comparable with Zhou et al. (2003), and Grzesik et al. (2017) [17], [18].

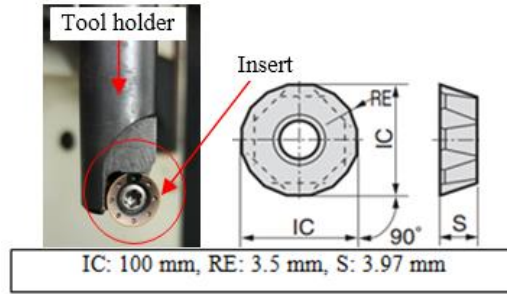


Figure 1: ball nose milling insert attached to the tool holder

Table 1: Workpiece chemical compositions

Workpiece Chemical compositions, % wt.	Ni:53.00	Cr:18.30	Fe:18.7	Nb:5.05	Cu:0.04
	Al:0.49	B:0.004	C:0.051	Co:0.3	P:<0.005
	Mo:3.05	Ti:1.05	Mn: 0.23	Si:0.08	S:<0.002

Table 2: Cutting parameters

Control parameters	Level of control parameters		
	-1	0	1
Cutting speed, $V_c$ (m/min)	120	130	140
Feed rate, $f_z$ (mm/tooth)	0.15	0.2	0.25
Axial DOC, $ap$ (mm)	0.3	0.5	0.7
Radial DOC, $ae$ (mm)	0.2	0.4	0.6

Figure 2 illustrates the experimental milling setup under the cryogenic condition and the Neo-MoMac system being used in this experiment. For the cryogenic cooling, the mixtures of CO<sub>2</sub> in the form of liquid and gas, together with compressed air, were used as the cryogen. The pressure of each coolant was controlled at 11 bar, 6 bar, and 4 bar for liquid CO<sub>2</sub>, gaseous CO<sub>2</sub>, and compressed air, respectively by the in-house designed of cryogenic CO<sub>2</sub> system as shown in Figure 2. The controlled minimum temperature of the mixed coolants from the nozzle is approximate -60 °C where the temperature consistency was confirmed by using a type-K thermometer. This cryogenic system is residue-free since the CO<sub>2</sub> will sublime at ambient temperature when it fuses with the ambient air.

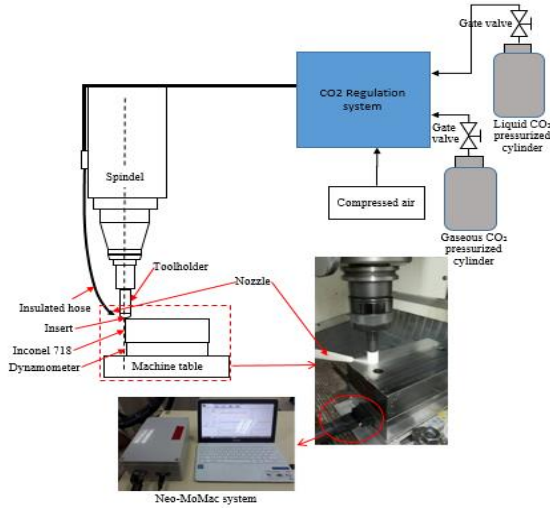


Figure 2: Experimental milling setup under cryogenic CO<sub>2</sub> and the Neo-MoMac system

## Result and Discussion

### Cutting force

The resultant forces ( $Fr$ ) were measured using the recorded cutting force components in x, y and z directions ( $F_x$ : tangential force,  $F_y$ : radial force and  $F_z$ : axial force) and Equation (1) [19]. The results are illustrated in Figure 3.

$$Fr = \sqrt{(F_x^2 + F_y^2 + F_z^2)} \quad (1)$$

The measured  $Fr$  varied from as low as 112 N up to a maximum of 452 N. The minimum  $Fr$  was achieved at  $V_c$ : 140 m/min,  $f_z$ : 0.2 mm/tooth,  $ap$ : 0.3 mm, and  $ae$ : 0.4 mm. Meanwhile, the maximum  $Fr$  was obtained at  $V_c$ : 130 m/min,  $f_z$ : 0.25 mm/tooth,  $ap$ : 0.7 mm and  $ae$ : 0.4 mm. When comparing the results to Musfirah et al. (2017) who also milled Inconel 718 but in cryogenic LN<sub>2</sub> condition, the  $Fr$  under cryogenic CO<sub>2</sub> could be considered as much lower [20]. This confirms the effectiveness of cryogenic CO<sub>2</sub> in reducing the cutting forces as also reported by Dilip and Pradeep (2012) and Cakir et al. (2014) [21][22]. The cryogenic cooling system provides consistent and adequate cooling effect deep into the cutting zone, mainly at the tool-chip interface for rapid heat dissipation from the cutting zone. It can be proved by the lesser cutting forces induced by the cutting

process as the results of less work hardening effect on the workpiece and lower temperature at the cutting edge by the flow of cryogenic CO<sub>2</sub>. This result is parallel to Patil et al. (2014) who pointed out that CO<sub>2</sub> managed to reduce the degree of work hardening of Inconel 718 even at the rapid generation of heat and temperatures at greater speeds and feed rates [5].

It can also be noted from Figure 3 that the tangential force ( $F_x$ ) has the major value, followed by the radial force ( $F_y$ ) and axial force ( $F_z$ ). The maximum  $F_x$  of 362.15 N was recorded at  $V_c$ : 130 m/min,  $f_z$ : 0.25 mm/tooth,  $ap$ : 0.7 mm and  $ae$ : 0.4 mm, while the minimum  $F_x$  of 50.40 N was at  $V_c$ : 130 m/min,  $f_z$ : 0.2 mm/tooth,  $ap$ : 0.3 mm and  $ae$ : 0.4mm. As found in this study, the  $F_x$  was found higher at higher cutting parameters where the volume of the workpiece to be removed increases as well. This increases the stress on the rake face of the tool, which is directly linked to the  $F_x$ . This result is in accordance with Kasim et al. (2018) who detailed the correlation between the material volume to be removed and the tangential force,  $F_x$  [23].

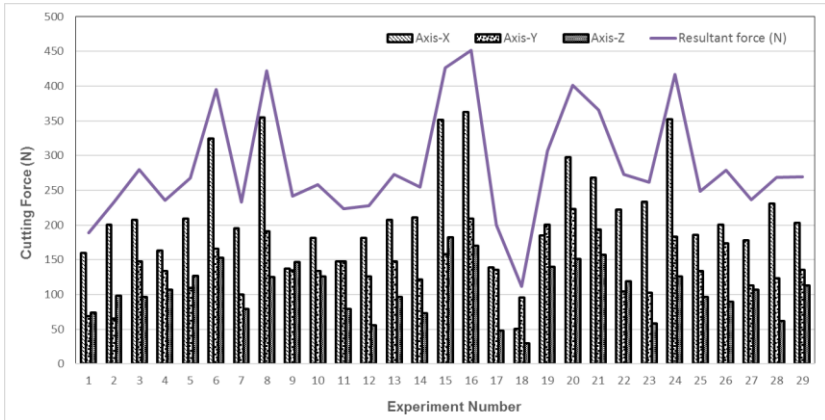


Figure 3: Cutting force results from 29 experiments

### Relationship between cutting force and tool wear

The progression of resultant force ( $F_r$ ) with the tool flank wear progress and pattern for experiment 16 is shown in Figure 4. At the beginning of the cut, the relationship was approximately linear, where the  $F_r$  increased gradually alongside flank wear progression. The tool wear pattern has shown the formation of abrasive wear and pitting along the cutting edge (at P1 and P2). This shows the high sensitivity of  $F_r$  with respect to the tool wear. As the wear progress increased, more energy was required to cut the material. The rapid increase of  $F_r$  occurred at tool wear of 0.1 mm onwards. Inconel 718, with high-temperature strength and very poor thermal conductivity, caused

low heat dissipation from the cutting zone. The heat that was accumulated at the cutting zone increased the cutting temperature and caused work hardening in the material. Thus, as the process continued, more shear strength was required to cut the material. The formation of build-up-edge (BUE) was also observed adhering at the cutting edge as in P3, P4, and P5. The BUE is referred to the welding of chips at the tool cutting edge in the excessive cutting temperatures. Its formation has an inverse effect on the tool performance and accelerates wear rate [24].

As shown in Figure 4, the highest  $F_r$  was achieved at the maximum tool flank wear (at P6). This is explained by the fact that at this point, the notch wear was developed and the tool cutting edge is not sharp enough to cut the material; thus, instead of cutting, it was pushing. This rubbing action consequence with higher  $F_r$  generated due to high shear strength and friction coefficient at tool-chip and tool-workpiece interfaces. Meanwhile, Wang et al. (2017) mentioned that a larger force is required to cut this material when machining at high speed [25]. A similar trend is also shown for the force components in the  $x$ ,  $y$ , and  $z$  directions. However, the majority of the force component is transmitted to the tool  $X$ -axis ( $F_x$ ) as also found by Kasim et al. (2015) [9].

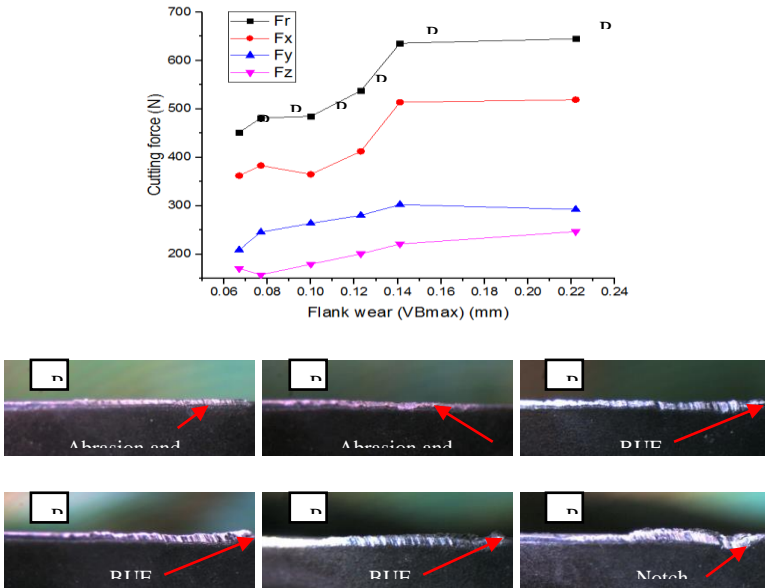


Figure 4: Progression of resultant forces with respect to tool flank wear progress and pattern for experiment 16 ( $V_c$ : 130 m/min,  $f_z$ : 0.25 mm/tooth,  $ap$ : 0.7 mm,  $ae$ : 0.4 mm)

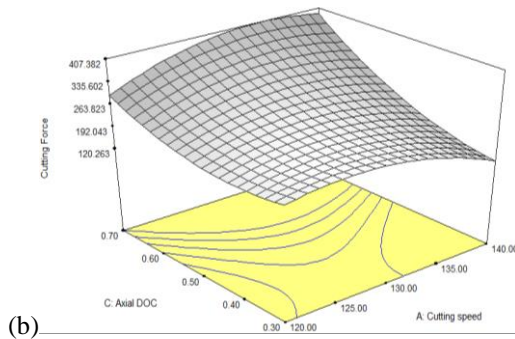
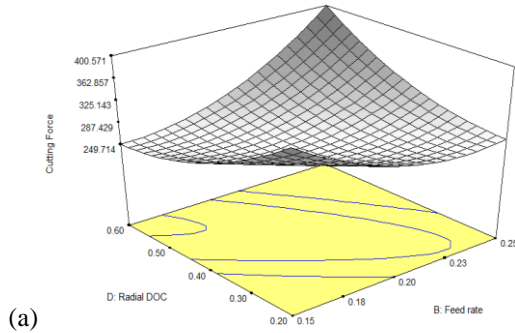
### Statistical analysis using ANOVA

Based on the ANOVA performed in Table 3, it shows that the F-Value of the model is 45.03 and the “Prob>F” is far less than 0.05. These values imply that the model is significant. For the significant factors, the Box-Behnken quadratic model obviously shows that factor C, A<sup>2</sup>, BD, C<sup>2</sup>, B<sup>2</sup>, AC, D<sup>2</sup>, AB, and B are the significant model terms in the model. All had Prob>F values larger than 0.05 and were listed in a descending order based on their respective values. These results revealed that the resultant force (*Fr*) in this machining process was majorly affected by axial DOC (*ap*). The increase of *ap* significantly increases the *Fr*. This is in line with the fact highlighted by Alauddin et al. (1998) who mentioned that it occurs due to the increase of the size of cut per tooth as the *ap* increases [12]. This is a consequence with the increase of the *Fr* required to produce the stress for deformation. The ANOVA also reveals that factors cutting speed (*Vc*) and radial DOC (*ae*) had no significant effect on the *Fr*. However; both factors were not removed from the analysis due to their interaction with other factors.

Table 3: ANOVA table for resultant force (*Fr*)

Source	Sum of squares	DF	Mean square	F Value	Prob> F	
Model	1.806x10 <sup>5</sup>	11	16420.35	45.03	< 0.0001	significant
A ( <i>Vc</i> )	66.82	1	66.82	0.18	0.6740	
B ( <i>fz</i> )	2225.07	1	2225.07	6.10	0.0244	
C ( <i>ap</i> )	94322.89	1	94322.89	258.68	< 0.0001	
D ( <i>ae</i> )	25.52	1	25.52	0.070	0.7945	
A <sup>2</sup>	20495.53	1	20495.53	56.21	< 0.0001	
B <sup>2</sup>	9179.08	1	9179.08	25.17	0.0001	
C <sup>2</sup>	15033.84	1	15033.84	41.23	< 0.0001	
D <sup>2</sup>	5319.72	1	5319.72	14.59	0.0014	
AB	1908.82	1	1908.82	5.23	0.0352	
AC	8359.72	1	8359.72	22.93	0.0002	
BD	15282.52	1	15282.52	41.91	< 0.0001	
Residual	6198.72	17	364.63			
Lack of Fit	4966.52	13	382.04	1.24	0.4572	not significant
R-Squared	0.9668					
Adj. R-Squared	0.9454					
Pred. R-Squared	0.8988					
Adeq. Precision	26.712					

Figures 5a, b and c illustrate the 3D surface model graphs of the  $Fr$  with different factorial interactions. Figure 5a shows the interaction between feed rate ( $fz$ ) and  $ae$ . The maximum  $Fr$  could be reached at the highest value of both factors (at  $fz$ : 0.25 mm/tooth and  $ae$ : 0.6 mm). It can then be minimized by reducing both factors to the lowest (at  $fz$ : 0.15 mm/tooth and  $ae$ : 0.2 mm). The interaction between  $Vc$  and  $ap$  is shown in Figure 5b. There is less significant effect on the  $Fr$  by the  $Vc$ . However, the minimum  $Fr$  can be obtained at the lowest  $ap$  (at 0.3 mm). As the  $ap$  and  $Vc$  increase, the  $Fr$  increases as well. The interaction between  $Vc$  and  $fz$  is shown in Figure 5c. The minimum  $Fr$  could be realized at the lowest value of  $Vc$  (at 120 m/min) and  $fz$  (at 0.15 mm/ tooth) and near the middle range of the  $fz$  (at 0.2 mm/tooth) and highest  $Vc$  (at 140 m/min).



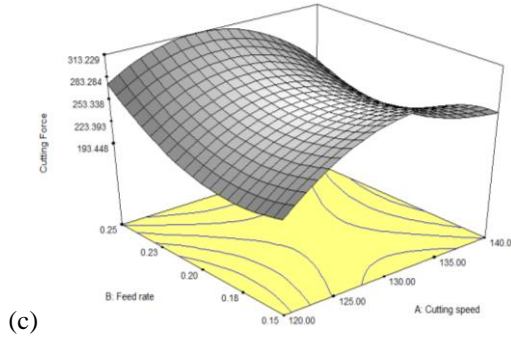


Figure 5: Interaction between; (a)  $fz$  and  $ae$  at  $Vc$  130 m/min and  $ap$  0.50 mm, (b)  $Vc$  and  $ap$  at  $fz$  0.2 mm/tooth and  $ae$  0.40 mm, and (c)  $Vc$  and  $fz$  at  $ap$  0.5 mm and  $ae$  0.40 mm

A second-order statistical equation model was developed by multiple regression and expressed in actual factors as shown in Equation (2). With the determination coefficient ( $R^2$ ) of the model as 0.9668 (as in Table 3), it specifies that the model adequately represents the real relationship between the variables and can be used to predict the value of  $Fr$ , within the limited range of the investigated parameters. Also shown in Table 3 that the lack of fit value is 0.4572, which indicates that the model is not significant; thus, it is fit and adequate for predicting the variation.

$$Fr = -3340.89 + 52.17Vc - 4068.43fz - 2931.78ap - 1816.27ae - 0.14Vc^2 + 15047.17fz^2 + 1203.57ap^2 + 715.95ae^2 - 21.85Vc.fz + 11.43Vc.ap + 6181.13fz.ae \quad (2)$$

### Model validation

In order to validate the adequacy of the model, the diagnostic plots of the normality plot, residuals vs. predicted, and randomness of the residual, as per Figure 6, needs to be analyzed. All of these proved that the residuals follow a normal distribution and fit the data well. As per Figure 6 (a), all the residuals fall close to the straight line, which means that the errors are distributed normally. Meanwhile, in Figure 6 (b) and (c), the data are within the limits, which showed no obvious pattern and unusual structure in the model. Further, Equation (2) was used to calculate the predicted values of resultant force for each experiment. The results were then compared with the actual experimental results to determine the accuracy of the model. Based on comparison results shown in Figure 7, the errors ranged from 0.03% to

10.54%, resulting in an average error of 4.72%. Since the average error is less than 10%, the model is considered acceptable to do the prediction [26].

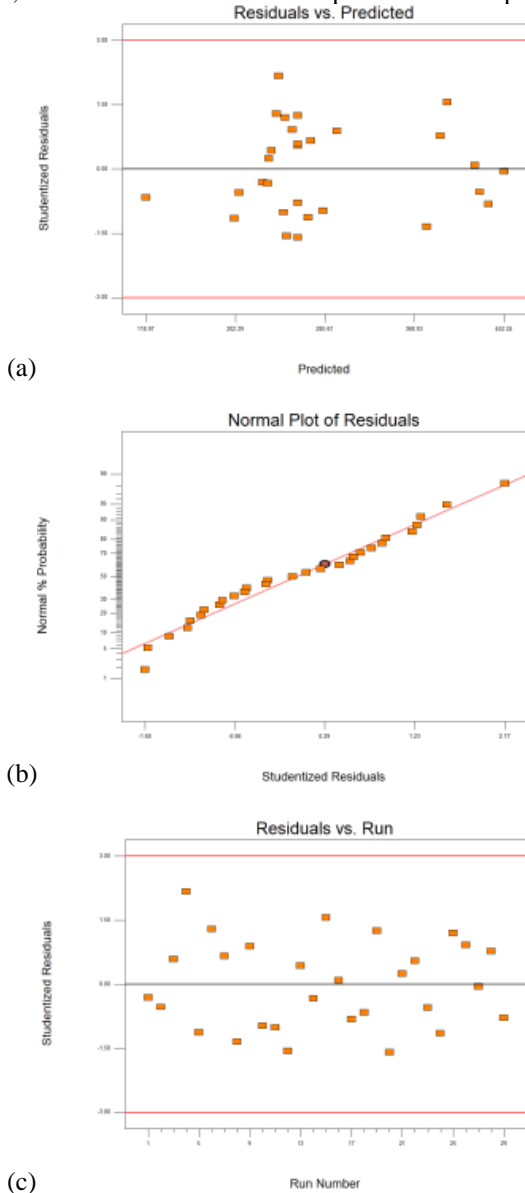


Figure 6: Residual plots of resultant force; (a) Normal plot of residuals, (b) Residuals vs. Predicted, and (c) Residuals vs. Run

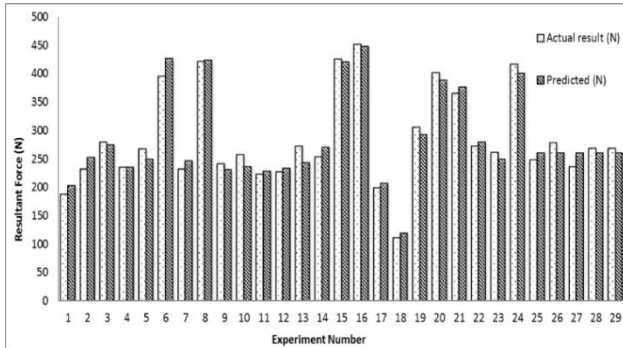


Figure 7: Comparison between actual and predicted resultant forces results

### Optimization of cutting force

For optimization, the lowest resultant force ( $Fr$ ) value of 117.72 N can be achieved at optimum parameters of  $V_c$ : 140 m/min,  $f_z$ : 0.25 mm/tooth,  $ap$ : 0.3 mm and  $ae$ : 0.21 mm. Perturbation plot as shown in Figure 8 was generated to exhibit how the optimized milling parameters interact with the  $Fr$ . As shown, the optimum  $Fr$  can be achieved at positive ends of factors A ( $V_c$ ) and B ( $f_z$ ), and at negative ends of factors C ( $ap$ ) and D ( $ae$ ). The steep slopes of the factors indicate the sensitivity of the force to each of them. The plot also shows a large decrease of the  $Fr$  as the factor C ( $ap$ ) decreases, which is in accordance with the prediction model that factor C ( $ap$ ) presents to be the most significant. These factors would further decrease the optimum value of the  $Fr$  by reducing their corresponding values.

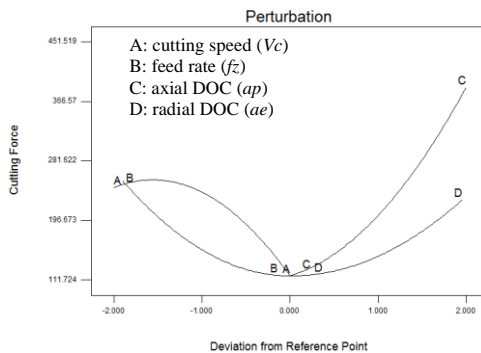


Figure 8: Perturbation plot of optimized cutting parameters for the resultant force

## Conclusion

In this study, the experimental design approach using Box Behnken RSM by Design Expert was successfully practiced in the optimization of cutting force in high-speed milling of Inconel 718 under cryogenic CO<sub>2</sub> condition. This study found that the resultant force ( $Fr$ ) values varied from as low as 112 N at  $V_c$ : 140 m/min,  $f_z$ : 0.2 mm/tooth,  $ap$ : 0.3 mm,  $ae$ : 0.4 mm to a maximum of 452 N at  $V_c$ : 130 m/min,  $f_z$ : 0.25 mm/tooth,  $ap$ : 0.7 mm,  $ae$ : 0.4 mm. These results evidence the effectiveness of cooling effect provided by the cryogenic CO<sub>2</sub> system to produce lower cutting force. From the ANOVA analysis, the results showed that the single factor of axial DOC ( $ap$ ) and interaction between the feed rate ( $f_z$ ) and radial DOC ( $ae$ ) were the most dominant factors influencing the  $Fr$ . Generally, the  $Fr$  increased as the  $ap$  and  $f_z$  increased. Also, the developed statistical equation model was found to accurately represent the  $Fr$  values, reporting only 4.72% average error when compared to the predicted and actual  $Fr$ . This shows that the model is adequate for predicting the  $Fr$  values within the range of investigated parameters. Meanwhile, the optimum parameters of  $V_c$ : 140 m/min,  $f_z$ : 0.25 mm/tooth,  $ap$ : 0.3 mm, and  $ae$ : 0.21 mm can be used to achieve a  $Fr$  as low as 117.72 N. It can, therefore, be concluded that the RSM under Box Behnken method is an efficient technique for analyzing the  $Fr$  trend in the context of various cutting parameters.

## References

- [1] A. Devillez, F. Schneider, S. Dominiak, D. Dudzinski, and D. Larrouquere, "Cutting forces and wear in dry machining of Inconel 718 with coated carbide tools," *Wear* 262 (7), pp. 931–942, 2007.
- [2] M. S. K. Musfirah, A.H., J. A. Ghani, C.H. Che Haron, "Effect of cutting parameters on cutting zone in cryogenic high speed milling of Inconel 718 alloy," *J. Teknol.* 77 (27), pp. 1–7, 2015.
- [3] C. Courbon, F. Pusavec, F. Dumont, J. Rech, and J. Kopac, "Tribological behaviour of Ti6Al4V and Inconel718 under dry and cryogenic conditions - Application to the context of machining with carbide tools," *Tribol. Int.* 66, pp. 72–82, 2013.
- [4] M. S. Kasim, C. H. Che Haron, J. A. Ghani, M. A. Sulaiman, and M. Z. A. Yazid, "Wear mechanism and notch wear location prediction model in ball nose end milling of Inconel 718," *Wear* 302 (1–2), pp. 1171–1179, 2013.
- [5] N. G. Patil, A. Asem, R. S. Pawade, D. G. Thakur, and P. K. Brahmanekar, "Comparative Study of High Speed Machining of Inconel 718 in Dry Condition and by Using Compressed Cold Carbon Dioxide Gas as Coolant," *Procedia CIRP* 24, pp. 86–91, 2014.

- [6] S. Zhang, J. F. Li, and Y. W. Wang, "Tool life and cutting forces in end milling Inconel 718 under dry and minimum quantity cooling lubrication cutting conditions," *J. Clean. Prod.* 32 (1), pp. 81–87, 2012.
- [7] Y. Kaynak, H. E. Karaca, R. D. Noebe, and I. S. Jawahir, "Analysis of Tool-wear and Cutting Force Components in Dry, Preheated, and Cryogenic Machining of NiTi Shape Memory Alloys," *Procedia CIRP* 8, pp. 498–503, 2013.
- [8] C. M. A.-C. Raymond H. Myers, Douglas C. Montgomery, *Response Surface Methodology - Process and Product Optimization using Designed Experiments*, Third. Canada: John Wiley & Sons, Inc., 2009.
- [9] M. Kasim, C. Haron, J. Ghani, N. Mohamad, R. Izamshah, M. Minhat, S. Mohamed, J. Saedon, and N. Saad, "Prediction of cutting force in end milling of Inconel 718," *J. Eng. Technol.* 5 (2), pp. 63–70, 2015.
- [10] N. Badroush, C. H. C. Haron, J. A. Ghani, M. F. Azhar, N. Hayati, and A. Halim, "Performance of Coated Carbide Tools when Turning Inconel Alloy 718 under Cryogenic Condition using RSM", *Journal of Mechanical Engineering* 5 (3), pp. 73–87, 2018.
- [11] S. L. Soo, R. C. Dewes, and D. K. Aspinwall, "3D FE modelling of high-speed ball nose end milling," *Int. J. Adv. Manuf. Technol.* 50 (9–12), pp. 871–882, 2010.
- [12] M. Alauddin, M. a. Mazid, M. a. El Baradi, and M. S. J. Hashmi, "Cutting forces in the end milling of Inconel 718," *J. Mater. Process. Technol.* 77 (1–3), pp. 153–159, 1998.
- [13] M. S. Said, J. a Ghani, M. S. Kassim, S. H. Tomadi, C. Hassan, and C. Haron, "Comparison between Taguchi Method and Response Surface Methodology ( RSM ) In Optimizing Machining Condition," *Int. Conf. Robust Qual. Eng.*, pp. 60–64, 2013.
- [14] K. Kadirgama, K. A. Abou-El-Hossein, B. Mohammad, H. Al-Ani, and M. M. Noor, "Cutting force prediction model by FEA and RSM when machining Hastelloy C-22HS with 90 holder," *J. Sci. Ind. Res. (India)*. 67 (6), pp. 421–427, 2008.
- [15] M. A. Hadi, J. A. Ghani, C. H. C. Haron, and M. S. Kasim, "Investigation on Wear Behavior and Chip Formation During Up-Milling and Down-Milling Operations for Inconel 718," *J. Teknol.* 3, pp. 15–21, 2014.
- [16] S. L. C. Ferreira, R. E. Bruns, H. S. Ferreira, G. D. Matos, J. M. David, G. C. Brandão, E. G. P. da Silva, L. A. Portugal, P. S. dos Reis, A. S. Souza, and W. N. L. dos Santos, "Box-Behnken design: An alternative for the optimization of analytical methods," *Anal. Chim. Acta* 597 (2), pp. 179–186, 2007.
- [17] J. M. Zhou, H. Walter, M. Andersson, and J. E. Stahl, "Effect of chamfer angle on wear of PCBN cutting tool," *Int. J. Mach. Tools Manuf.* 43 (3), pp. 301–305, 2003.

- [18] W. Grzesik, P. Nieslony, W. Habrat, J. Sieniawski, and P. Laskowski, "Investigation of tool wear in the turning of Inconel 718 superalloy in terms of process performance and productivity enhancement," *Tribol. Int.*, 2017.
- [19] M. Alauddin, M. a. El Baradie, and M. S. J. Hashmi, "Modelling of cutting force in end milling Inconel 718," *J. Mater. Process. Technol.* 58 (1), pp. 100–108, 1996.
- [20] A. H. Musfirah, J. A. Ghani, and C. H. C. Haron, "Tool wear and surface integrity of inconel 718 in dry and cryogenic coolant at high cutting speed," *Wear* 376–377, pp. 125–133, 2017.
- [21] B. Dilip Jerold and M. Pradeep Kumar, "Experimental comparison of carbon-dioxide and liquid nitrogen cryogenic coolants in turning of AISI 1045 steel," *Cryogenics (Guildf)*. 52 (10), pp. 569–574, 2012.
- [22] O. Çakır, M. Kıyak, and E. Altan, "Comparison of gases applications to wet and dry cuttings in turning," *J. Mater. Process. Technol.* 153, pp. 35–41, 2004.
- [23] M. Kasim, C. Che Haron, J. A. Ghani, R. Izamshah, M. Akmal, M. A. Ali, M. Hadzley, and M. S. Salleh, "Investigation of tangential force on ball nose rake face during high-speed milling of Inconel 718," *Adv. Mater. Process. Technol.* 698, pp. 1–7, 2018.
- [24] Y. S. Liao, H. M. Lin, and J. H. Wang, "Behaviors of end milling Inconel 718 superalloy by cemented carbide tools," *J. Mater. Process. Technol.* 201 (1–3), pp. 460–465, 2008.
- [25] F. Wang, L. Li, J. Liu, and Q. Shu, "Research on tool wear of milling nickel-based superalloy in cryogenic," *Int. J. Adv. Manuf. Technol.*, pp. 1–10, 2017.
- [26] R. Hills and T. Trucano, *Statistical validation of engineering and scientific models: Background*, 1999.